THE JOURNAL OF PHYSICAL CHEMISTRY C

Article

pubs.acs.org/JPCC

Spatially Resolved Transport Properties of Pristine and Doped Single-Walled Carbon Nanotube Networks

Andrej Znidarsic,[†] Antti Kaskela,[‡] Patrik Laiho,[‡] Miran Gaberscek,[†] Yutaka Ohno,[§] Albert G. Nasibulin,[‡] Esko I. Kauppinen,[‡] and Abdou Hassanien*,[†]

[†]Electrochemical Materials Department, National Institute of Chemistry, 19 Hajdrihova, Ljubljana 1000, Slovenia

[‡]Nanomaterials Group, Department of Applied Physics, School of Science, Aalto University, P.O. Box 15100, 00076, Aalto, Finland

[§]Department of Quantum Engineering, Nagoya University, Nagoya 464-8603, Japan

Supporting Information

ABSTRACT: We use noninvasive atomic force microscopy to probe the spatial electrical conductivity of isolated junctions of pristine and nitric acid treated single-walled carbon nanotube networks (SWCNT-N). By analyzing the local IV curves of SWCNTs and bundles with various diameters, the resistance per unit length and the contact resistance of their junctions are estimated to be 3−16 kΩ/μm and 29−532 kΩ, respectively. We find that the contact resistance decreases with increasing SWCNT or bundle diameter and depends on the contact morphology, reaching a value of 29 kΩ at a diameter of 10 nm. A nitric acid treatment moderately dopes SWCNTs and reduces their average contact resistance by a factor of 3 while the resistance of the nanotubes remains largely unaltered. Remarkably, the same treatment on an SWCNT-N shows similar reduction in the sheet resistance by a factor of 4. These results suggest that the resistance reduction mechanism is related to the contact modulation with no major impact on conductance of SWCNTs.

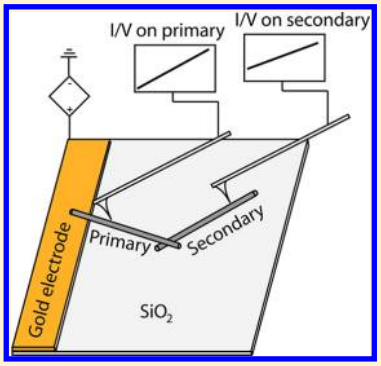

1. INTRODUCTION

Single-walled carbon nanotube networks (SWCNT-N) are of great interest for many application areas that utilize transparent conductive films[1] and would benefit from flexibility and high transparency, such as flat panel displays,[2] touch sensors,[3] solar cell electrodes,[4] etc. As ∼1/3 of the aerosol-CVD nanotubes are metallic and ∼2/3 are semiconducting, low-density SWCNT-Ns are required for high-performance thin film transistors (TFTs).[5−7] At high densities, metallic nanotubes form metallic pathways between the source and the drain electrodes, leading to a poor response to gate modulation. SWCNT-Ns are an appealing material for such applications since the network properties are determined by aggregate behavior of the network elements. That means, these properties are averaged over a large number of individual nanotubes, which reduces the required degree of control over individual nanotube properties. For a realistic SWCNT-N, the important performance-impacting parameters are related to the morphology of the network, defined by the mean bundle or nanotube length and diameter, the network density, junction fill factor, bundle alignment, etc. Previous work with low-density films for SWCNT-TFTs has highlighted the significance of controlling morphological parameters, especially the junction fill factor and nanotube alignment, for device properties, such as their on/off ratio and mobility.[8] In networks suitable for SWCNT thin conducting film (SWCNT-TCF) applications, the network density is significantly higher and the bundle length has been identified to be the most important parameter for TCF performance, which is determined by electrical sheet resistance and optical transmittance.[6] The major impact of bundle length for SWCNT-TCF performance is explained by reduction in the number of interbundle and intertube contacts, which are expected to dominate the overall resistance of typical SWCNT-Ns.[9−12] Earlier experimental[12] and theoretical[13−15] works have given insight into the charge transport across individual SWCNTs junctions, but the details of the microscopic properties and their effects on electronic properties of the interface region remained unexplored. More recently, the local transport properties of individual junctions have been studied;[11] however, liquid-based sample fabrication introduces defects and/or increases the risk of residual impurities at the contact interface. Although the use of surfactants to disperse SWCNTs has allowed their separation by both type and chirality, there is no assurance that they can be completely removed with a mild treatment, which complicates local transport measurements.

The other approach of studying SWCNT-N transport is to study macroscopic thin films. Several studies suggest that their performance can be improved by various chemical dopants.[16,17] However, little is known about the details of the doping process and how it affects the electronic properties of SWCNTs and their individual contacts. To address these issues, we study the microscopic charge transport properties of individual contacts, before and after doping, to investigate conditions under which

Received: April 22, 2013
Revised: May 28, 2013
Published: June 5, 2013

   dx.doi.org/10.1021/jp403983y | J. Phys. Chem. C 2013, 117, 13324−13330

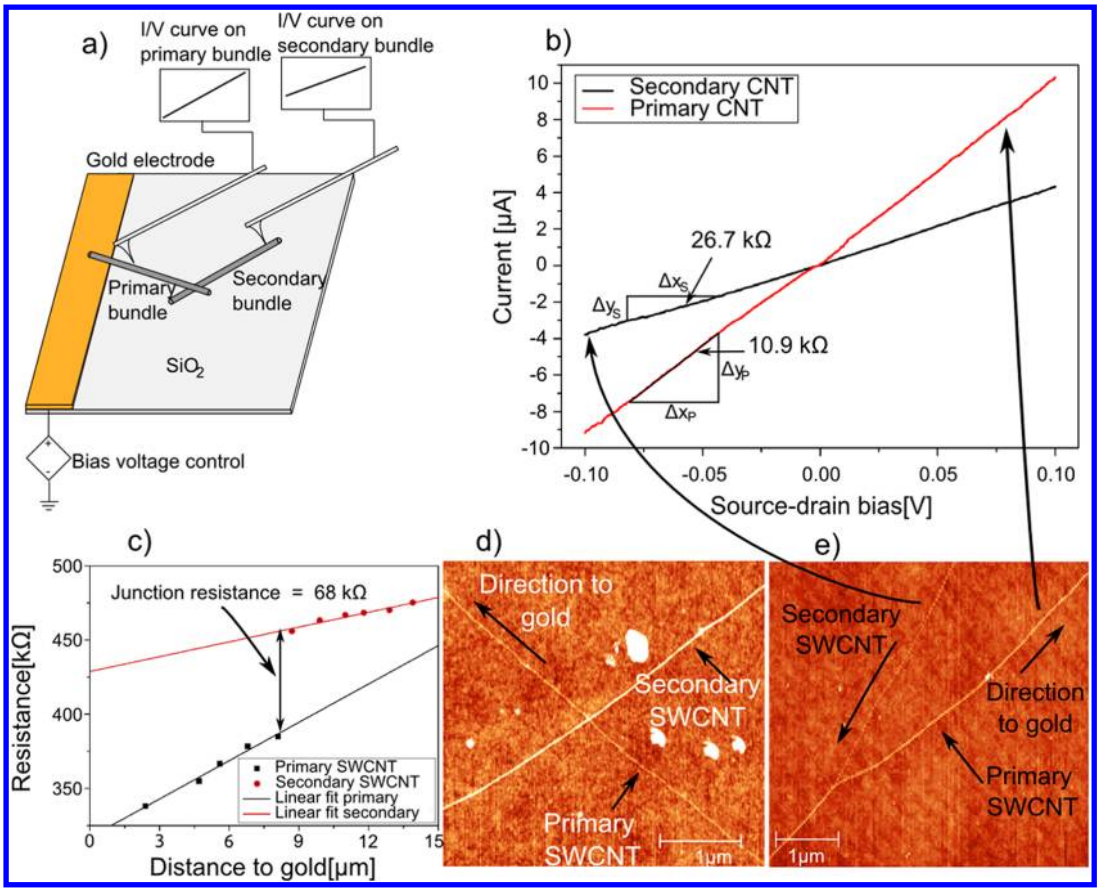

Figure 1. Local electrical properties of SWCNT intermolecular junction. (a) Measurement layout: A combination between tapping and contact mode is used to image and probe the local electrical properties of isolated SWCNT junctions near the Au contacts. (b, c) Tapping mode images of X and Y junctions. (d) Resistance profile across an individual intermolecular junction.

SWCNT-TCF will yield high-performance devices. The pristine SWCNT material of this study is prepared by a floating catalyst aerosol-CVD method that yields dispersed and high-quality SWCNTs. Clean and low-density SWCNT-N samples for both thin film and microscopic charge transport studies are fabricated by utilizing a dry deposition method at room temperature.[5,6,18] These pristine SWCNT materials have not been processed in any way prior to electrical transport and spectroscopic measurements. The samples are then subjected to a nitric acid treatment (1−2 min), and the measurements are repeated to explore the variation in the individual contact and the thin film properties. On the basis of local electrical measurements, we find that the nitric acid treatment does not introduce major defects or changes in SWCNT mobility. However, the average resistance of individual contacts and the sheet resistance are reduced by a factor of 3 and 4, respectively. The improved performance, of the SWCNT-TCF after the nitric acid treatment, is explained in terms of lowering the average barrier height between contacts of individual tubes as a result of hole-doping.

2. EXPERIMENTAL SECTION

2.1. SWCNT Synthesis. The SWCNT samples used in this study were prepared by a floating catalyst aerosol-CVD process, which is described in detail elsewhere.[19] In brief, the process relies on sublimation of ferrocene to a carbon monoxide (CO) flow, injection of the gases to a vertical laminar flow synthesis reactor, thermal decomposition of ferrocene to supersaturated iron vapor, and subsequent formation of catalyst iron nanoparticles. In the synthesis reactor, which is maintained at elevated temperatures, the CO reacts catalytically on the surface of the catalysts, leading to SWCNT formation. In these experiments, a semi-industrial scale synthesis reactor was operated at a temperature of 880 °C.[6] A trace amount of 20 ccm of CO_2 was added to the CO flow of 4 L/min (lpm) to enhance the catalytic activity of the reaction.[20] At the reactor outlet, the aerosol was mixed with a 80 lpm flow of room-temperature N_2 to reduce the gas temperature to be compatible with the used collection filters.

2.2. Sample Preparation. SWCNTs were collected downstream from the reactor by utilizing membrane filtration, which allows straightforward control of SWCNT network thickness, and electrical and optical properties, by varying the collection time, using the same procedure described in previous publications.[6,21] In this study, the films were press transferred to microscope glass slides, and ethanol-densified to improve SWCNT network adhesion. To study the impact of chemical doping, the films were submerged for 1 min in a strong nitric acid solution (Sigma-Aldrich, 68 vol %).[6] For C-AFM characterization of spatially resolved electrical properties, SWCNTs were deposited by a diffusion method on SiO_2 (250 nm) substrates (Si-Mat) with prefabricated gold electrodes (40 nm thick Au layer on 5 nm Ti, with p^{++} Si as a back gate) by placing the chips directly on top of a membrane filter during collection. This leads to deposition of very sparse SWCNT networks with isolated SWCNT contacts, some of which were connected to the gold electrode. The device layout

dx.doi.org/10.1021/jp403983y | J. Phys. Chem. C 2013, 117, 13324−13330

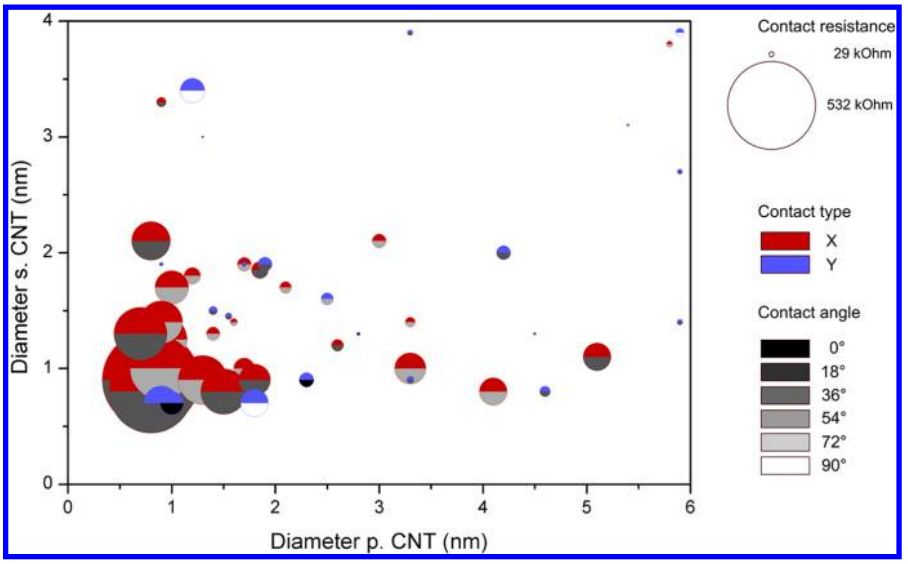

Figure 2. Contact resistance of X and Y junctions vs diameters of primary and secondary CNTs and their intersecting angles. Y junctions have smaller resistances than X junctions at any given structural parameter with a minimum value of 29 kΩ. The contact resistance of both junctions is inversely proportional to the diameters of CNT branches.

and measurement configuration are shown schematically in Figure 1.

2.3. C-AFM Measurement Setup. The C-AFM measurements (Veeco Multimode V, Veeco, USA/Nanonis, Specs, Switzerland) are carried out at room temperature in an ambient pressure environmentally controlled chamber of 6.5l in volume flushed with a flow of 99.99% of argon (Scientific Argon produced by Messer, Slovenia and Aga, Finland) at constant flow rate of 0.2 L/min. During measurement of IV curves, the doped diamond tip (Nanosensors DT-NCHR, Nanoworld AG, Switzerland) was brought into contact at a constant force of 0.2 nN. Resistances per unit length were estimated by performing IV curve measurements at different points with approximately 1 μm of separation along an SWCNT. The intertube and interbundle contact resistances were estimated based on differential measurement over various junctions, so that IV curves were recorded at 0.5 μm distances from the contact on both branches to avoid contact modification by tip pressure. The C-AFM tip cleanliness was checked on Au electrodes before and after collecting data on SWCNTs to ensure the reliability of IV characterization by requiring contact tip−electrode contact resistance < 8 kΩ and by checking the linearity of the IV curves. The AFM imaging was carried out by conventional tapping mode while electrical measurements were performed under constant force in AFM contact mode. Prior to contact, a slow approach soft landing was performed. Unlike previous C-AFM contact resistance measurements on SWCNT samples, this approach allows the tip to avoid jumping into contact, which has a high risk of damaging the SWCNT.[22] IV measurements were performed by ramping the source drain bias from −3 to +3 V, while monitoring the source−drain current.

3. RESULTS AND DISCUSSION

3.1. Characterization of Individual SWCNTs contacts. The microscopic transport properties in SWCNT-Ns are studied using conductive atomic force microscopy (C-AFM) for combined imaging and probing the local physical properties of intertube and interbundle contact resistance, tube resistance per unit length, diameter, and contact angle between intersecting SWCNTs (or bundles).

To perform local electrical transport measurements on individual junctions, it is necessary to prepare low-density SWCNT samples with isolated junctions near the Au electrode. An important consideration is paid to the sample fabrication process, so we can obtain reliably highly dispersed pristine SWCNTs without the need for any chemical processing. A schematic layout of the local IV measurements is shown in Figure 1a, which we have used to monitor resistance at various locations on SWCNTs; see Figure 1b. X or Y junctions are characterized by recording the resistance profile along both branches of SWCNT junctions. The diameter of each SWCNT is determined from the line profile of the AFM topographic image. As illustrated in Figure 1c, the contact of two SWCNTs with diameters of 1.3 and 1.4 nm yields a resistance of 68 kΩ. Figure 1d,e displays the two main morphologies of SWCNT intermolecular junctions: an "X-type" junction and a "Y-type" junction. To avoid complex current flow from AFM tip to Au electrode through multiple connected SWCNTs, measurements were carried out only on junctions where both of SWCNTs or SWCNT bundles were isolated from other SWCNTs, as verified by AFM imaging of the surrounding area. We denote the SWCNT or bundle that is directly connected to the Au electrode as the primary branch and the other SWCNT or bundle connected to the primary branch as the secondary branch. Each of these branches can be either an individual single-walled carbon nanotube (SWCNT) or a small bundle of SWCNTs that is generally a mix of semiconducting and metallic species.

Figure 2 shows the contact resistance (R_j) as a function of primary and secondary SWCNT and bundle diameters and the intersecting angles (θ) for a number of X- and Y-type junctions. All contact resistances of SWCNTs, with diameters from 1 to 10 nm, are found within a range from 29 to 532 kΩ. Y-type junctions exhibit a significantly lower contact resistance than X-type junctions, and the resistance decreases with increasing bundle diameter. The behavior of contact resistance with the diameter of SWCNTs is in contrast with a previous study by Nirmalraj et al., which suggested that SWCNT junction

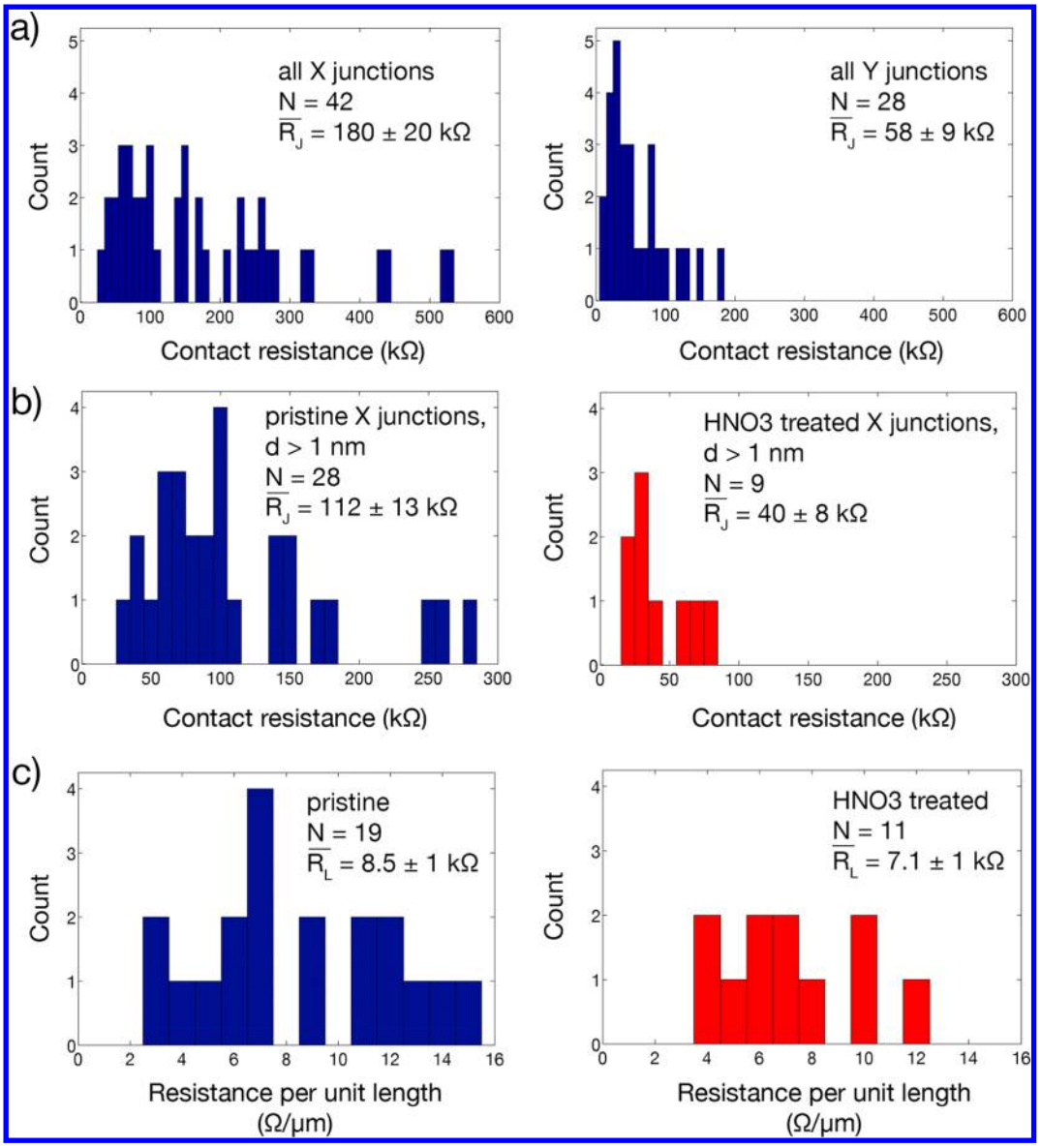

Figure 3. (a) The overall contact resistance of X-type and Y-type contacts suggests that the Y-type contacts have a lower contact resistance compared to X-type contacts. (b) The X-type contacts for $d > 1$ nm tubes and bundles show significant reduction of sheet resistance after HNO_3 doping. (c) However, the resistance per unit length is only slightly reduced.

resistance is directly proportional to the diameter of SWCNTs.[11] It is worth noting that they observed mainly large-diameter SWCNT bundles, and the difference between the experiments could be explained by the presence of SDS surfactant or other residual contaminants in their SWCNT samples, whereas this is not the case with our surfactant-free deposition. Moreover, high contact resistances (>100 kΩ) are only observed in X junctions with small-diameter SWCNTs that form Schottky-type contacts. Their existence within SWCNT-N is undesirable as they limit the film conductance and may cause local accumulation of heat, thereby triggering SWCNT-N device breakdown at a relatively low power.[23] Previous theoretical works[24,25] have shown that the conductance of Schottky-type contact increases dramatically by a hole-doping process due to reduction in the width of the depletion region as well as the barrier height. As pristine SWCNTs are already hole-doped with a density of $\sim 10^{-3}$ hole/atom due to atmospheric oxygen physisorption,[26−29] the depletion region of the Schottky contact will be negligibly small.[25] Furthermore, hole-doping also decreases the barrier height by shifting the Fermi level toward the valence band, and therefore, the contact resistance will be more reduced. Generally, this is achieved by chemically treating SWCNTs with nitric or sulfuric acid, a process that is known to downshift the Fermi level by 0.35 and 0.50 eV, respectively.[30] We have prepared moderately doped samples by dipping SWCNT-N films briefly in nitric acid (Sigma Aldrich, 68% HNO_3). Figure 3a shows a histogram of the contact resistance for all X (left) and all Y (right) junctions that we have measured in our study. A comparison between the contact resistance of the X junction before and after treatment is shown in Figure 3b. The average contact resistance is reduced by a factor of ∼3, indicating improved barrier transmissions after nitric acid treatment. It has been argued by Geng et al. that the increase in conductivity of SWCNT-N after treatment is not related to doping, but rather due to densification and the removal of the SDS surfactant in the case of solution-processed SWCNTs,[16] whereas other papers have concluded that it may be due to improvement of

dx.doi.org/10.1021/jp403983y | J. Phys. Chem. C 2013, 117, 13324−13330

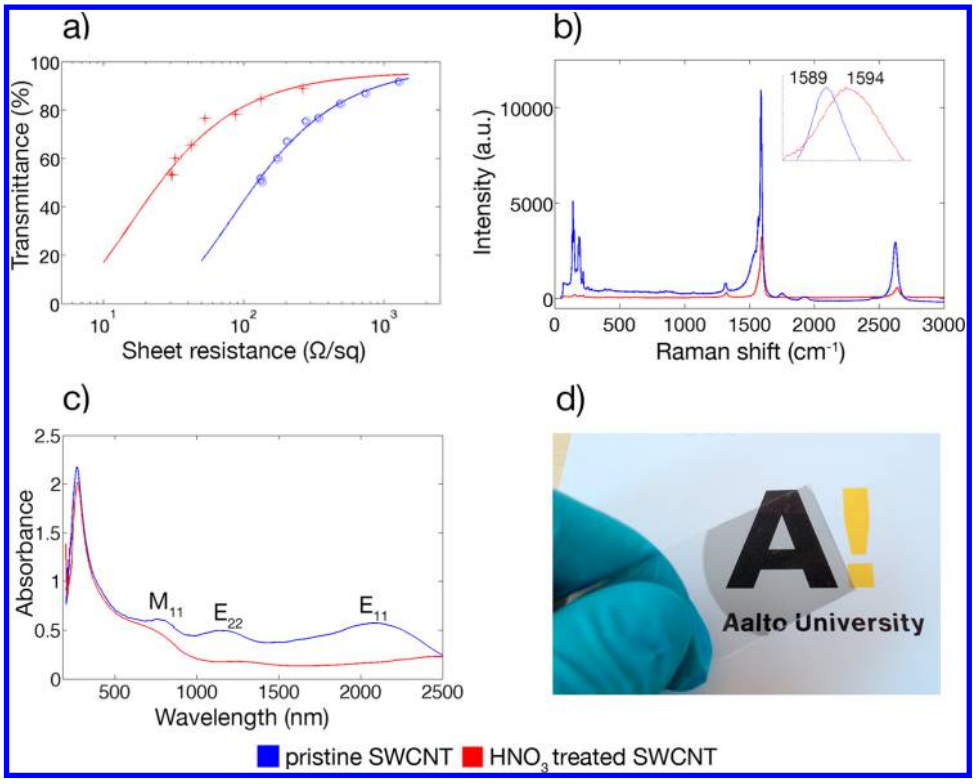

Figure 4. (a) Sheet resistance and transmittance of pristine, ethanol-densified films and HNO_3-doped SWCNT TCF samples with different collection times. The acid treatment leads to significant reduction of sheet resistance by a factor of 4. (b) Raman spectrum of pristine and doped SWCNT films indicates upshift in G-band, overall intensity reduction, and high G/D ratio after the doping treatment, indicating a small amount of doping-induced defects. (c) The pristine SWCNT network exhibits clear semiconductive tube related transitions E_{11} and E_{22}, which are suppressed due to the acid treatment. (d) Optical image of a transparent SWCNT-TCF on a glass substrate demonstrates the transparency of the SWCNT-TCF.

conductivity of individual SWCNTs and junctions.[11,31−33] We have measured the resistance per unit length before and after doping for a number of SWCNTs, and the results are shown in Figure 3c. This asserts that doping mainly lowers the contact resistance between SWCNTs. This is in agreement with Raman spectroscopic analysis of pristine and doped SWCNT-Ns (Figure 4b), which shows that the high G/D ratio remains largely unchanged after the treatment, thus confirming that the quality of SWCNTs is still preserved. The Raman-spectroscopic sample characterization was carried out with a 633 nm incident laser wavelength (Horiba Jobin-Yvon, Labram HR). The observed upshift of the G-band peak position and reduction of the overall Raman signal intensity have been linked to hole-doping via charge transfer between the dopants and the SWCNTs.[16,34] The lowered RBM intensity can be explained in terms of variations in the resonance condition as the Fermi level shifts its position toward the valence band.[29] Therefore, we conclude that the acid treatment improves the overall conductivity of SWCNTs by lowering the barrier height without introducing a significant number of structural defects, such as covalently bonded functional groups.

3.2. Network Characterization. The SWCNT-TCFs were characterized by electrical four-point probe measurements and optical characterization with UV−vis spectroscopy for determination of optical transmittance and SWCNT diameter, and for verification of chemical doping. Furthermore, Raman spectroscopy was used for analysis of chemical doping effects and potential SWCNT quality degradation after acid treatment. We start by rinsing films in ethanol, a common process that is known to lower the resistance by improving the connectivity of the network. The films were then dried at room temperature prior to been investigated by electrical and optical techniques. The electrical transport measurement obtained for ethanol-densified films exhibits a sheet resistance of about ∼400 Ω/sq at 80% transmittance. After the nitric acid treatment, we find that films are hole-doped as the overall Raman signal intensity is reduced with an upshift in the G and G' bands' position. Despite the rapid treatment, the films are having improved performance with the sheet resistance decreasing to 100 Ω/sq at 80% transmittance which corresponds to a reduction by a factor of 4, as shown in the Figure 4a. Moreover, the semiconducting optical transitions of pristine films are completely suppressed after doping, thereby yielding a slightly higher overall transmission of films after nitric acid treatment. We now discuss the microscopic origin of improved performance after hole-doping of SWCNT-TCF by considering local transport data obtained from C-AFM measurements.

The micro- and macroscale resistance characterizations can be linked by modeling an SWCNT-N as a random network of resistors. The resistance between two parallel cross-sectional edges of a square segment of such a network, that is, sheet resistance, is linearly dependent on the mean contact resistance. This indicates that doping-induced changes in contact resistances should be observable also in the macroscopic sheet resistance.[23] When also taking into account the resistance along SWCNTs, and using the measured values for contact resistance and resistance per unit length from pristine (R_C = 112 ± 13 kΩ, R_L = 8.7 ± 1 kΩ/μm) and HNO_3-treated (R_C = 40 ± 8 kΩ, R_L = 7.1 ± 1 kΩ/μm) samples in an equivalent circuit model, the sheet resistance (for networks of similar

dx.doi.org/10.1021/jp403983y | J. Phys. Chem. C 2013, 117, 13324−13330

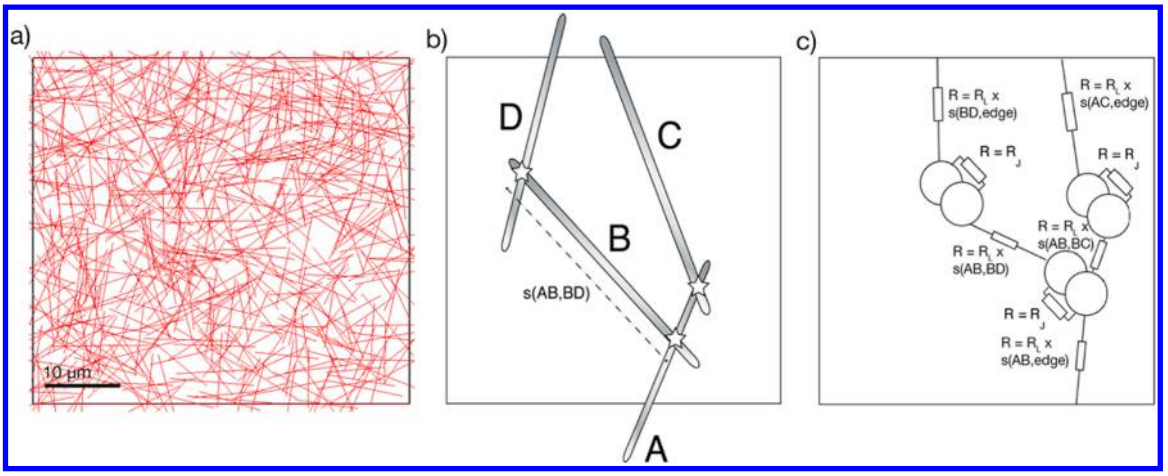

Figure 5. The impact of nitric acid treatment to overall TCF performance is studied computationally by an equivalent resistor network model depicted schematically here. (b) A simple network of four line segments, representing the SWCNTs. The intersection points and the Euclidean distance s(AB, BD) between two of the intersection points have been marked. (c) An equivalent circuit formed from the network. At each intersection point, two nodes are placed. A resistor with the measured junction resistance R_J is placed between each node pair sharing the same coordinates, and a resistor with a resistance equaling the resistance per unit length, multiplied by the Euclidean distance s, between adjacent nodes on the same wire.

densities) was reduced by a factor of 1.7 (Figure 5). The change after doping in the simulated network is lower compared to observed changes in SWCNT-TCF sheet resistance, where the similar doping treatment reduced the sheet resistance by a factor of 4×. It should be noted that the input parameters of the model consist only of contact resistance measurements from pristine and doped X-type junctions and length resistance measurements from small-diameter structures. Thus, the contact and length resistances used as the model's input parameters may differ from realistic contact and length resistances of the transparent conductive films, which consist typically of larger-diameter bundles[6] and contain a fraction of Y-type junctions. Accounting for these effects could well explain the discrepancy between the modeled and measured sheet resistances and suggests that they should be studied further.

4. CONCLUSION

To summarize, we have performed spatially resolved C-AFM measurements of pristine and acid-treated SWCNTs to estimate their resistances per unit length and contact resistances between bundles. High contact angle, X-type contacts were found to exhibit larger contact resistances than low contact angle, Y-type contacts. The diameters of connected SWCNTs or SWCNT bundles are observed to have a dominant role in determining the overall contact resistance. The contact resistances were significantly reduced—by a factor of ∼3—after a rapid nitric acid treatment. These results compare favorably with electrical measurements on films, which show that sheet resistances are reduced by a factor of 4 after a similar treatment. The difference between the extremely sparse C-AFM samples and more dense TCF samples can be explained by the fact that contact resistances were measured only between small-diameter bundles and individual nanotubes with X-type junctions, whereas the bundle diameters in typical SWCNT films are typically larger and have a fraction of Y-type junctions. Also, it is worth noting that the acid treatment may cause a change to the junction type (from X- to Y-type) and increase bundle diameters and thus modulate the TCF network performance by favorable morphological changes in addition to hole-doping. The nitric acid treatment has no major impact on the resistance per unit length of individual tubes, indicating that no appreciable change in defect density or structure degradation has occurred. This verifies that the electrical performance improvement is due to the increase in charge density of CNTs and the reduction of barrier height of high resistance contacts. The potential for improved performance as a result of the doping process requires additional effort to realize its advantages in transparent electronic applications. These efforts should be devoted to controlling key parameters, such as dopant concentration, aging, and morphological changes (densification), while maintaining the quality of the SWCNTs intact. The effect of the nitric acid treatment to contact and length resistance should be generalizable to other dopants, since similar effects have been observed in TCFs for various dopants, including nitric, hydrochloric, and sulphuric acids,[30] thionyl chloride,[16] and potassium permanganete in acidic solution.

■ ASSOCIATED CONTENT

Ⓢ Supporting Information

SEM images are showing the morphologies of pristine and acid-treated carbon nanotube thin film networks and conducting AFM samples. This material is available free of charge via the Internet at http://pubs.acs.org.

■ AUTHOR INFORMATION

Corresponding Author

*E-mail: abdou.hassanien@ki.si.

Notes

The authors declare no competing financial interest.

■ ACKNOWLEDGMENTS

The financial support from the Centre of Excellence Low Carbon Technologies (CO NOT) is fully acknowledged. We would like to thank Ahmed Kreta for help with C-AFM experiments at the final stage of this project.

■ REFERENCES

(1) Wu, Z.; Chen, Z.; Du, X.; Logan, J. M.; Sippel, J.; Nikolou, M.; Kamaras, K.; Reynolds, J. R.; Tanner, D. B.; Hebard.; et al.

Transparent, Conductive Carbon Nanotube Films. *Science* **2004**, *305*, 1273−1276.
(2) Wang, C.; Zhang, J.; Ryu, K.; Badmaev, A.; De Arco, L. G.; Zhou, C. Wafer-Scale Fabrication of Separated Carbon Nanotube Thin-Film Transistors for Display Applications. *Nano Lett.* **2009**, *9*, 4285−4291.
(3) Choi, E.; Kim, J.; Chun, S.; Kim, A.; Lee, K.; Jeong, M.; Lim, C.; Isoshima, T.; Hara, M.; Lee, S. B. Fabrication of a Flexible and Transparent Touch Sensor Using Single-Walled Carbon Nanotube Thin-Films. *J. Nanosci. Nanotechnol.* **2011**, *11*, 5845−5849.
(4) Rowell, M. W.; Topinka, M. A.; McGehee, M. D.; Prall, H.-J.; Dennler, G.; Sariciftci, N. S.; Hu, L.; Gruner, G. Organic Solar Cells with Carbon Nanotube Network Electrodes. *Appl. Phys. Lett.* **2006**, *88*, 233506.
(5) Sun, D. M.; Timmermans, M. Y.; Tian, Y.; Nasibulin, A. G.; Kauppinen, E. I.; Kishimoto, S.; Mizutani, T.; Ohno, Y. Flexible High-Performance Cabon Nanotube Integrated Circuits. *Nat. Nanotechnol.* **2011**, *6*, 156−161.
(6) Kaskela, A.; Nasibulin, A. G.; Timmermans, M. Y.; Aitchison, B.; Papadimitratos, A.; Tian, Y.; Zhu, Z.; Jiang, H.; Brown, D. P.; Zakhidov.; et al. Aerosol-Synthesized SWCNT Networks with Tunable Conductivity and Transparency by a Dry Transfer Technique. *Nano Lett.* **2010**, *10*, 4349−4355.
(7) Cao, Q.; Rogers, J. A. Ultrathin Films of Single-Walled Carbon Nanotubes for Electronics and Sensors: A Review of Fundamental and Applied Aspects. *Adv. Mater.* **2009**, *21*, 29−53.
(8) Timmermans, M. Y.; Estrada, D.; Nasibulin, A. G.; Wood, J. D.; Behnam, A.; Sun, D.-m.; Ohno, Y.; Lyding, J. W.; Hassanien, A.; Pop, E.; Kauppinen, E. I. . Effect of Carbon Nanotube Network Morphology on Thin Film Transistor Performance. *Nano Res.* **2012**, *5*, 307−319.
(9) Harris, J. M.; Iyer, G. R.; Bernhardt, A. K.; Huh, J. Y.; Hudson, S. D.; Fagan, J. A.; Hobbie, E. K. Electronic Durability of Flexible Transparent Films from Type-Specific Single-Wall Carbon Nanotubes. *ACS Nano* **2012**, *6*, 881−887.
(10) Stadermann, M.; Papadakis, S. J.; Falvo, M. R.; Novak, J.; Snow, E.; Fu, Q.; Liu, J.; Fridman, Y.; Boland, J. J.; Superfine, R.; Washburn, S. Nanoscale Study of Conduction Through Carbon Nanotube Networks. *Phys. Rev. B* **2004**, *69*, 201402.
(11) Nirmalraj, P. N.; Lyons, P. E.; De, S.; Coleman, J. N.; Boland, J. J. Electrical Conductivity in Single-Walled Carbon Nanotube Networks. *Nano Lett.* **2009**, *9*, 3890−3895.
(12) Fuhrer, M. S.; Nygard, J.; Shih, L.; Forero, M.; Yoon, Y. G.; Mazzoni, M. S.; Choi, H. J.; Ihm, J.; Louie, S. G.; Zettl, A.; et al. Crossed Nanotube Junctions. *Science* **2000**, *288*, 494−497.
(13) Léonard, F.; Tersoff, J. Role of Fermi-Level Pinning in Nanotube Schottky Diodes. *Phys. Rev. Lett.* **2000**, *84*, 4693−4696.
(14) Nakanishi, T.; Ando, T. Conductance of Crossed Carbon Nanotubes. *J. Phys. Soc. Jpn.* **2001**, *70*, 1647−1658.
(15) Odintsov, A. A. Schottky Barriers in Carbon Nanotube Heterojunctions. *Phys. Rev. Lett.* **2000**, *85*, 150−153.
(16) Geng, H. Z.; Kim, K. K.; So, K. P.; Lee, Y. S.; Chang, Y.; Lee, Y. H. Effect of Acid Treatment on Carbon Nanotube-Based Flexible Transparent Conducting Films. *J. Am. Chem. Soc.* **2007**, *129*, 7758−7759.
(17) Parekh, B. B.; Fanchini, G.; Eda, G.; Chhowalla, M. Improved Conductivity of Transparent Single-Wall Carbon Nanotube Thin Films via Stable Postdeposition Functionalization. *Appl. Phys. Lett.* **2007**, *90*, 121913.
(18) Nasibulin, A. G.; Kaskela, A.; Mustonen, K.; Anisimov, A. S.; Ruiz, V.; Kivistö, S.; Rackauskas, S.; Timmermans, M. Y.; Pudas, M.; Aitchison.; et al. Multifunctional Free-Standing Single-Walled Carbon Nanotubes. *ACS Nano* **2011**, *5*, 3214−3221.
(19) Moisala, A.; Nasibulin, A. G.; Brown, D. P.; Jiang, H.; Khriachtchev, L.; Kauppinen, E. I. Single-Walled Carbon Nanotube Synthesis Using Ferrocene and Iron Pentacarbonyl in a Laminar Flow Reactor. *Chem. Eng. Sci.* **2006**, *61*, 4393−4402.
(20) Nasibulin, A. G.; Brown, D. P.; Queipo, P.; Gonzalez, D.; Jiang, H.; Kauppinen, E. I. An Essential Role of CO_2 and H_2O During Single-Walled CNT Synthesis From Carbon Monoxide. *Chem. Phys. Lett.* **2006**, *417*, 179−184.
(21) Nasibulin, A. G.; Ollikainen, A.; Anisimov, A. S.; Brown, D. P.; Pikhitsa, P. V.; Holopainen, S.; Penttilä, J. S.; Helistö, P.; Ruokolainen, J.; Choi.; et al. Integration of Single-Walled Carbon Nanotubes into Polymer Films by Thermo-Compression. *Chem. Eng. J.* **2008**, *136*, 409−413.
(22) Kovic, A.; Znidarsic, A.; Jesih, A.; Mrzel, A.; Gaberscek, M.; Hassanien, A. A Novel Facile Synthesis and Characterization of Molybdenum Nanowires. *Nanoscale Res. Lett.* **2012**, *7*, 567.
(23) Estrada, D.; Pop, E. Imaging Dissipation and Hot Spots in Carbon Nanotube Network Transistors. *Appl. Phys. Lett.* **2011**, *98*, 073102.
(24) Léonard, F.; Tersoff, J. Novel Length Scales in Nanotube DevicesJ. *Phys. Rev. Lett.* **1999**, *83*, 5174−5177.
(25) Havu, P.; Hashemi, M. J.; Kaukonen, M.; Seppala, E. T.; Nieminen, R. M. Effect of Gating and Pressure on the Electronic Transport Properties of Crossed Nanotube Junctions: Formation of a Schottky Barrier. *J. Phys.: Condens. Matter* **2011**, *23*, 112203.
(26) Martel, R.; Schmidt, T.; Shea, H. R.; Hertel, T.; Avouris, P. Single- and Multi-Wall Carbon Nanotube Field Effect Transistors. *Appl. Phys. Lett.* **1998**, *73*, 2447−2449.
(27) Collins, P. G.; Bradley, K.; Ishigami, M.; Zettl, A. Extreme Oxygen Sensitivity of Electronic Properties of Carbon Nanotubes. *Science* **2000**, *287*, 1801−1804.
(28) Kong, J.; Franklin, N. R.; Zhou, C.; Chapline, M. G.; Peng, S.; Cho, K.; Dai, H. Nanotube Molecular Wires as Chemical Sensors. *Science* **2000**, *287*, 622−625.
(29) Sumanasekera, G. U.; Adu, C. K.; Fang, S.; Eklund, P. C. Effects of Gas Adsorption and Collisions on Electrical Transport in Single-Walled Carbon Nanotubes. *Phys. Rev. Lett.* **2000**, *85*, 1096−1099.
(30) Zhou, W.; Vavro, J.; Nemes, N. M.; Fischer, J. E.; Borondics, F.; Kamarás, K.; Tanner, D. B. Charge Transfer and Fermi Level Shift in *p*-Doped Single-Walled Carbon Nanotubes. *Phys. Rev. B* **2005**, *71*, 205423−205429.
(31) Graupner, R.; Abraham, J.; Vencelová, A.; Seyller, T.; Hennrich, F.; Kappes, M. M.; Hirsch, A.; Ley, L. Doping of Single-Walled Carbon Nanotube Bundles by Brønsted Acids. *Phys. Chem. Chem. Phys.* **2003**, *5*, 5472−5476.
(32) Skákalová, V.; Kaiser, A. B.; Dettlaff-Weglikowska, U.; Hrncariková, K.; Roth, S. Effect of Chemical Treatment on Electrical Conductivity, Infrared Absorption, and Raman Spectra of Single-Walled Carbon Nanotube Networks. *J. Phys. Chem. B* **2005**, *109*, 7174−7181.
(33) Chandra, B.; Afzali, A.; Khare, N.; El-Ashry, M. M.; Tulevski, G. S. Single Charge-Transfer Doping of Transparent Single-Walled Carbon Nanotube Films. *Chem. Mater.* **2010**, *22*, 5179−5183.
(34) Lee, R. S.; Kim, H. J.; Fischer, J. E.; Thess, A.; Smalley, R. E. Conductivity Enhancement in Single-Walled Carbon Nanotube Bundles Doped with K and Br. *Nature* **1997**, *388*, 255−257.